Journal of Biomechanics 96 (2019) 109335

Contents lists available at ScienceDirect

Journal of Biomechanics

journal homepage: www.elsevier.com/locate/jbiomech
www.JBiomech.com

Regional distribution of layer-specific circumferential residual deformations and opening angles in the porcine aorta

Dimitrios P. Sokolis *

Laboratory of Biomechanics, Center of Clinical, Experimental Surgery, and Translational Research, Biomedical Research Foundation of the Academy of Athens, Athens, Greece

ARTICLE INFO

Article history:
Accepted 8 September 2019

Keywords:
Layer separation
Residual stretch
Bending
Zero-stress state
Aorta

ABSTRACT

Information on the layer-specific residual deformations of aortic tissue and how these vary throughout the vessel is important for understanding the regionally-varying aortic functions and pathophysiology, but not so much can be found in the literature. Toward this end, porcine aortas were sectioned into eighteen rings, with one ring from each anatomical position radially cut to obtain the zero-stress state for the intact wall and the other ring dissected into intimal-medial and adventitial layers; these rings were then radially cut to reach the zero-stress state for the intima-media and adventitia. Peripheral variations in internal/external circumferences, thickness, and opening angle of the intact wall and its layers were measured through image analysis at the no-load and zero-stress states. Intact wall and layer circumferences at both states significantly declined along the aorta, as did intact wall and intimal-medial but not adventitial thickness. Adventitia exhibited the greatest opening angles, approaching 180 deg all over the aorta. The opening angles of the intima-media and intact wall were quite similar, with the highest values in the ascending aorta, the lowest at the diaphragm, and increasing subsequently. Bending-related residual stretches were released by radial cutting that were compressive internally and tensile externally, displaying distinct axial variation for the intima-media and intact wall, and non-significant variation for the adventitia. Evidence is provided for the release upon layer separation of compressive stretches in the intima-media and of tensile stretches in the adventitia, whose values were smallest in the descending thoracic aorta and highest near the iliac artery bifurcation.

1. Introduction

Knowledge of the biomechanical properties of the aortic wall and of their variation with axial position is important for an in-depth understanding of the numerous aortic functions, namely the central coupling with the heart and the peripheral coupling with the tissues and organs of the body, as well as for appreciating the regionally-varying pathophysiology, namely the susceptibility to aortic dissection proximally and to atherosclerotic disease and abdominal aortic aneurysm distally (Boudoulas and Wooley, 1996; Nichols et al., 2011). In this regard, constitutive modeling of physiologic, pathophysiologic, and traumatic conditions is urgently needed, requiring information about the zero-stress state of the aorta (Humphrey, 2002).

Based on the pioneering investigations by Chuong and Fung (1986) and by Vaishnav and Vossoughi (1987), it is now customarily assumed that the zero-stress state of an artery is not a closed cylinder free of external loads, but rather a radially cut-open sector. The variation of this geometry along the arterial tree has been characterized (Han and Fung, 1991), reporting opening angle data as an indication of the magnitude of circumferential residual strains, and our group lately afforded a comprehensive regional distribution of opening angle and residual strains for the human aorta (Sokolis et al., 2017). However, a single radial cut does not relieve all the residual stresses in an unloaded ring, as has been discussed in the seminal review article by Rachev and Greenwald (2003). In particular, Vossoughi et al. (1993) reported that by cutting an aortic ring into outer and inner rings, the opening angle associated with each radially-cut part was dissimilar, an observation corroborated by the detailed experiments of Greenwald et al. (1997). A smaller opening angle was found for the outer rings and a larger was found for the inner rings, but these rings did not associate with individual wall layers.

Since the aortic wall consists of intima, media, and adventitia, it is meaningful to examine the zero-stress state of the individual layers, but very little information is available in the pertinent literature. Holzapfel et al. (2007) provided the first layer-specific residual strain data for the human infrarenal aorta and Peña et al. (2015)

* Address: 35, Lefkados St., Athens 15354, Greece.
E-mail address: DimitrisSokolis@ath.forthnet.gr

https://doi.org/10.1016/j.jbiomech.2019.109335
0021-9290/

reported layer-specific opening angles for the porcine descending aorta. The regional variation of layer-specific residual strains along the aorta appears to be unknown however. Accordingly, the purpose of this communication was to determine the axial distribution of the layer-specific circumferential residual deformations and opening angles over the length of the porcine aorta. Given the thinness of the intima in young laboratory animals, the combined intima-media and the adventitia were the two basic layers examined.

2. Material and methods

2.1. Biological tissue and sample preparation

Full-length aortas, from the coronary arteries to the iliac artery bifurcation, were obtained in one piece from ten female Landrace pigs weighing 65 kg that were used in other unrelated physiological studies. The aortas were removed immediately after euthanasia and stored for a maximum of 2 h in 0.9% saline solution at room temperature. Adjoining connective tissues were gently cleaned from the aortas and they were divided into nine successive segments: (1) ascending thoracic aorta; (2) beginning and (3) end of the aortic arch; (4) upper, (5) middle, and (6) lower descending thoracic aorta; as well as (7) upper, (8) middle, and (9) lower abdominal aorta. Fixed locations along the aorta were used as reference for axial anatomical position; that is the two aortic arch segments were taken before and after the aortic arch branches; the middle descending thoracic segment was demarcated by the 3rd and 7th pair of intercostal arteries. The abdominal aorta was cut into three sections of equal length, at the level of the celiac, renal, and inferior mesenteric arteries. A pair of neighboring rings with ~5-mm length was transversely cut from each aortic segment, avoiding large-branch vessel orifices, i.e., stress concentration sites caused by naturally occurring perforations, by a distance of at least 3 mm. One of the rings from each pair was radially cut to obtain the zero-stress state for the intact wall, whereas the other ring was dissected into intimal-medial and adventitial layers with the aid of a stereomicroscope (Nikon SMZ800; Nikon Instruments Europe BV) and a digital camera (Leica DFC500; Leica Microsystems GmbH). These rings were then radially cut to reach the zero-stress state for the intima-media and adventitia.

The medial and adventitial layers were distinguished based on visual appearance and texture, as in past studies from our laboratory, e.g. (Sokolis, 2015). A more reddish color was assigned to the adventitia due to the presence of vasa vasorum, whereas the media exhibited a rather yellowish color due to elastin and a more cohesive texture. A scalpel was moved circularly above the adventitial aspect of the aortic rings, thereby exerting small shear forces and causing separation of the adventitia at some point. Separation beyond that point was achieved by carefully pulling apart the

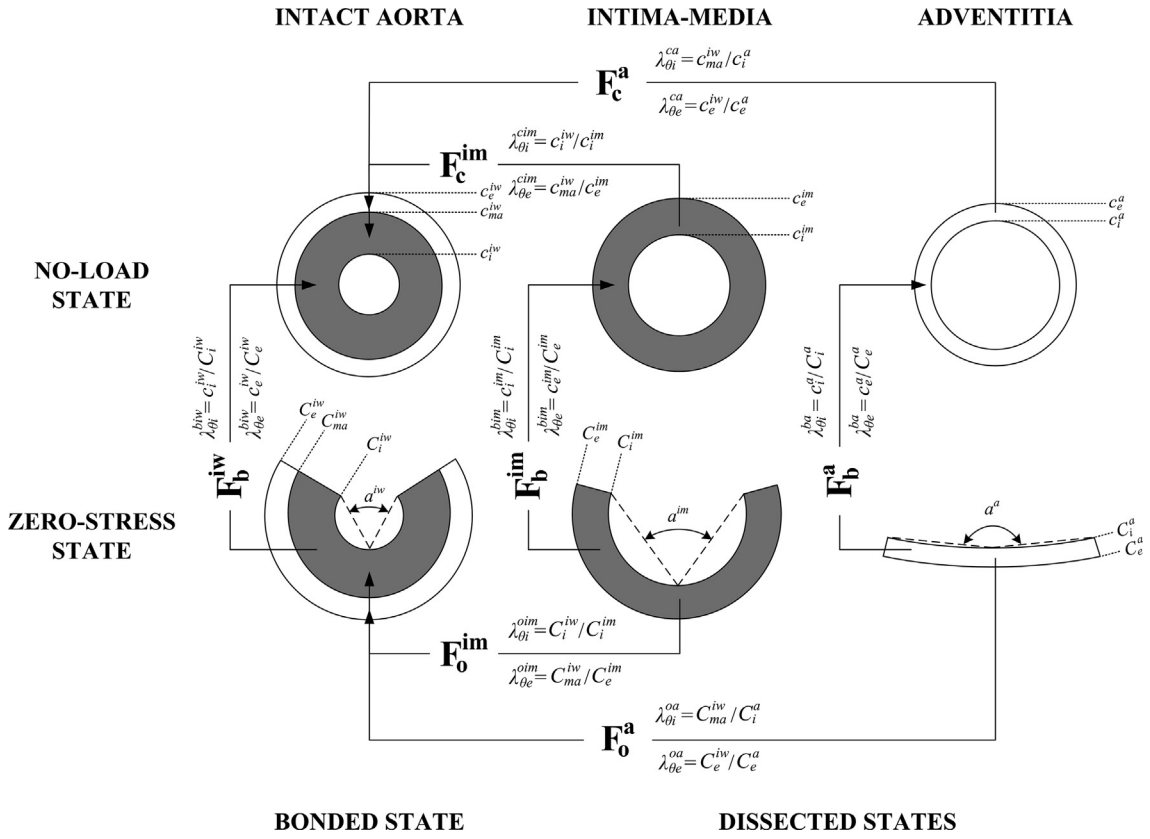

Fig. 1. Cross-sectional geometric representation of the intact wall (denoted by superscript iw, bonded state) and of its basic layers (dissected states), i.e., the intima-media (denoted by superscript im) and adventitia (denoted by superscript a), at the no-load state (upper panel) and the zero-stress state (lower panel). The opening angle, denoted by *a*, i.e., the most common descriptor of residual strains, is the angle subtended by two radii connecting the midpoint of the internal wall to the sector tips. *C* and *c* denote in turn the circumferences at the zero-stress state and the no-load state. The circumferential (denoted by subscript θ) residual stretch at the internal surface, denoted by subscript *i*, (or at the external surface; denoted by subscript *e*) relating with the opening up of the arc sector after the radial cut was calculated as the internal (or the external) circumference at no-load divided by that at zero-stress; see the formulae and the associated deformation gradients $\mathbf{F}_\mathbf{b}^\mathbf{iw}$, $\mathbf{F}_\mathbf{b}^\mathbf{im}$, $\mathbf{F}_\mathbf{b}^\mathbf{a}$ for the intact wall, intima-media, and adventitia (denoted by subscript b, i.e., bending-related). The residual stretch at the internal (or external) surface of the intima-media and adventitia relating to layer dissection was calculated as the internal circumference and that at the interface between the two layers (or as the external circumference) of the intact wall divided by the internal (or external) circumference of the two layers; see the formulae and the deformation gradients $\mathbf{F}_\mathbf{o}^\mathbf{im}$ and $\mathbf{F}_\mathbf{o}^\mathbf{a}$ for the intima-media and adventitia at the zero-stress state (denoted by subscript o, i.e., radially cut-open) in addition to the deformation gradients $\mathbf{F}_\mathbf{c}^\mathbf{im}$ and $\mathbf{F}_\mathbf{c}^\mathbf{a}$ at the no-load state (denoted by subscript c, i.e., closed ring).

two layers with microsurgical nippers until the adventitia was securely detached from the media along the full circumference of the ring. In case a ring opened during layer dissection or the intended layer included part of the other layer (as macroscopically visualized or sporadically identified via histology), additional rings were dissected. These were available in the descending thoracic and abdominal aorta that usually yielded more than the twelve rings required. Histological preparation, i.e., formalin-fixation, paraffin-embedding, and staining with hematoxylin-eosin and Sirius red, was conducted on some radially-cut rings to substantiate the correctness of layer separation.

2.2. Bending-related and layer-specific residual stretch determination

The intact wall rings and those for the separated layers were arranged in Petri dishes and their cross-sections photographed at the no-load (closed) and zero-stress (radially-cut open) states under near-passive smooth muscle tone. Morphometric parameters (external and internal circumferences of the rings, and their minimum, maximum, and mean thicknesses) were measured from the digitized photographs at the two states. A thorough description of our experimental and analytical procedures is given in §S.2.1. and §S.2.2. (Supplementary Material). The following circumferential residual stretches were calculated from the morphometric parameters: (1) the external and internal residual stretches pertaining to the opening up of the sector after the radial cut ($\lambda_{\theta e}^{biw}$, $\lambda_{\theta i}^{biw}$ for the intact wall, $\lambda_{\theta e}^{bim}$, $\lambda_{\theta i}^{bim}$ for the intima-media, and $\lambda_{\theta e}^{ba}$, $\lambda_{\theta i}^{ba}$ for the adventitia); (2) those released in the intima-media ($\lambda_{\theta e}^{cim}$, $\lambda_{\theta i}^{cim}$) and adventitia ($\lambda_{\theta e}^{ca}$, $\lambda_{\theta i}^{ca}$) upon separation at the no-load state; and (3) those released in the intima-media ($\lambda_{\theta e}^{oim}$, $\lambda_{\theta i}^{oim}$) and adventitia ($\lambda_{\theta e}^{oa}$, $\lambda_{\theta i}^{oa}$) upon separation at the zero-stress state; see the residual stretch definitions and associated kinematics in Fig. 1.

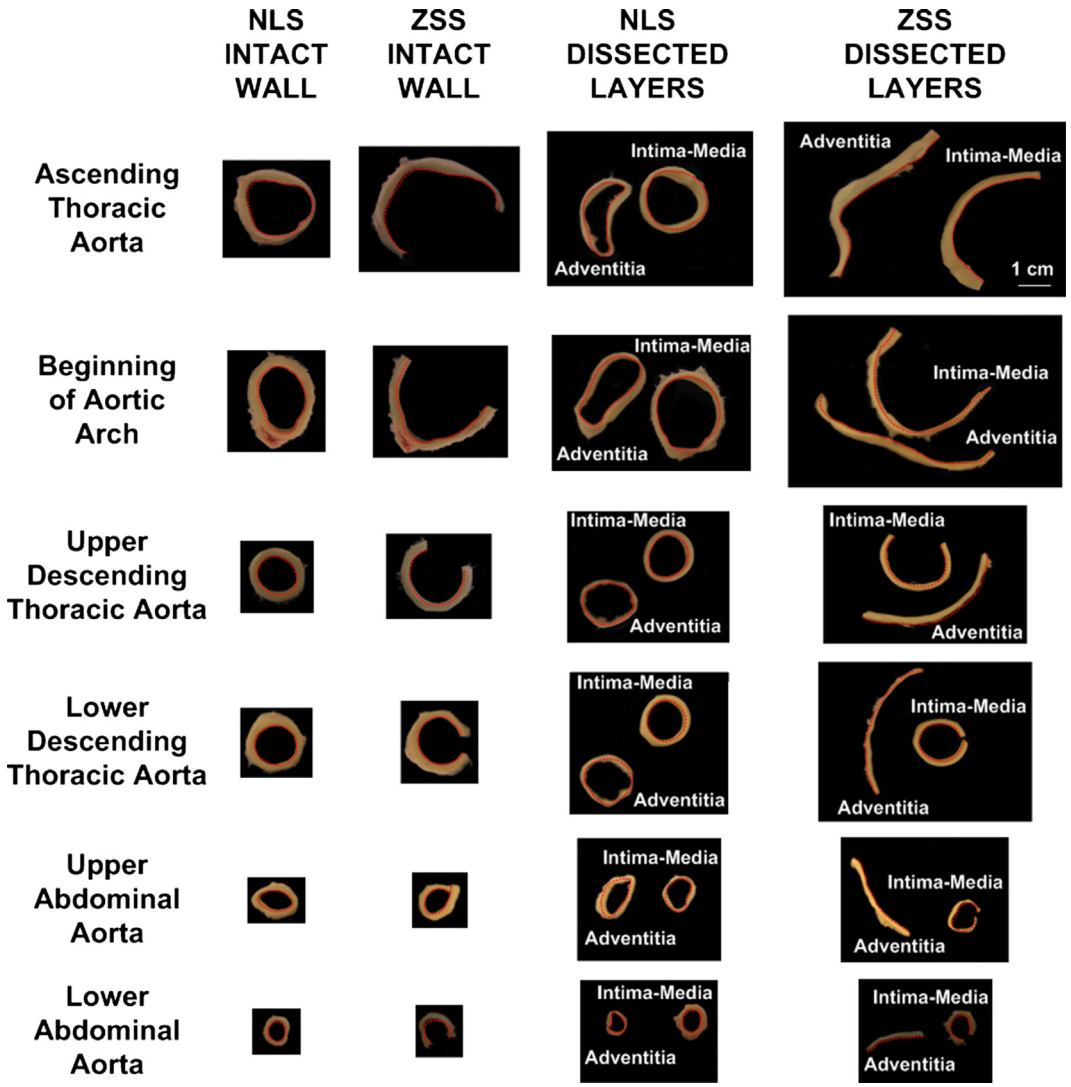

Fig. 2. Photographs of intact aortic wall and separated layer rings at their no-load state (NLS) and their zero-stress state (ZSS), as obtained from six distinct anatomical positions. Each row of photographs corresponds to the anatomical position indicated on the left hand side and the four columns correspond in turn to the NLS (first column) and ZSS (second column) of the intact aortic wall rings, and to the NLS (third column) and ZSS (fourth column) of the separated intimal-medial and adventitial rings. The red dotted curves mark the internal boundaries of the rings and radially-cut specimens. During the experiments, each ring was photographed, along with a mm scale, before and after being submitted to radial cutting as well as after layer separation and radial cutting. This mm scale has been omitted for clarity (instead a single scale bar is shown applying to all the photographs). The labeling used for referencing the intact wall and separated layer rings, and their open configurations has also been omitted for clarity, but the intima-media and adventitia are designated in all the photographs of the separated layers. (For interpretation of the references to color in this figure legend, the reader is referred to the web version of this article.)

2.3. Statistics

One-way analysis of variance (ANOVA) for repeated measures and the Tukey post hoc test were performed for multiple comparisons between anatomical positions in the intact wall, intima-media, and adventitia, as well as between the two layers and the intact wall in a given position. Statistical comparisons between the no-load and zero-stress states, as well as between the external and internal residual stretches in a given position were performed with the paired *t*-test. Significance was defined at $p < 0.05$. SPSS v18.0 (SPSS Inc, Chicago, IL, USA) was used.

The reproducibility of our method for hand-tracing wall boundaries and measuring opening angles was tested in thirty random zero-stress state images, using the coefficient of variation (=standard deviation expressed as percent of the mean of serial measurements). 4.8 ± 1.4% was the mean intra-observer coefficient during ten blinded internal circumference measurements of the adventitia, and 3.3 ± 1.2% the mean inter-observer coefficient during five measurements by independent observers (the author and a student). The respective values for the opening angle measurement were 4.9 ± 2.4% and 4.4 ± 2.1%. Better were the results for the intima-media and intact wall.

3. Results

3.1. Macroscopic and histological observations

Cross-sectional views of the intact aortic wall and the separated layers at their no-load and zero-stress states are shown in Fig. 2 for different anatomical positions. Characteristic histological sections are presented in Fig. 3, certifying mostly atraumatic layer separation. Note the comparable opening of the radially-cut rings in fresh and histologically-processed tissue from each anatomical position.

3.2. Aortic wall and layer circumferences at various positions

The external and internal circumferences varied with anatomical position along the aorta (Fig. 4). As regards the intact wall and intima-media, the greatest external and internal circumferences at both the no-load and zero-stress states were found in the beginning of the aortic arch. These values decreased slightly towards the ascending aorta, decreasing more abruptly in the direction of blood flow. By contrast, the greatest circumferences of the adventitia were observed in the ascending aorta, decreasing along the arch, increasing little along the upper descending thoracic aorta only as regards the zero-stress state values and then decreasing to a minimum in the lower abdominal aorta.

Results of the statistical analyses are summarized in Fig. 4. Highly significant variation with anatomical position was present in the circumferences of both the intact wall and its layers at their individual no-load and zero-stress states. The internal circumference of the intact wall was significantly smaller at the no-load compared with the zero-stress state, unlike its external circumference that was significantly greater and led to the bending-related residual stretches. Similar differences between the no-load and zero-stress states were found for the intima-media, whereas those for the adventitia were found in fewer positions. The external circumference of the separated adventitia was consistently smaller than that when the two layers were attached to the intact wall, considering either the no-load or zero-stress states, unlike the internal circumference of the intima-media. These differences mirror the layer-specific residual stretches identified, noting that only the internal and external boundaries of the layers and the intact

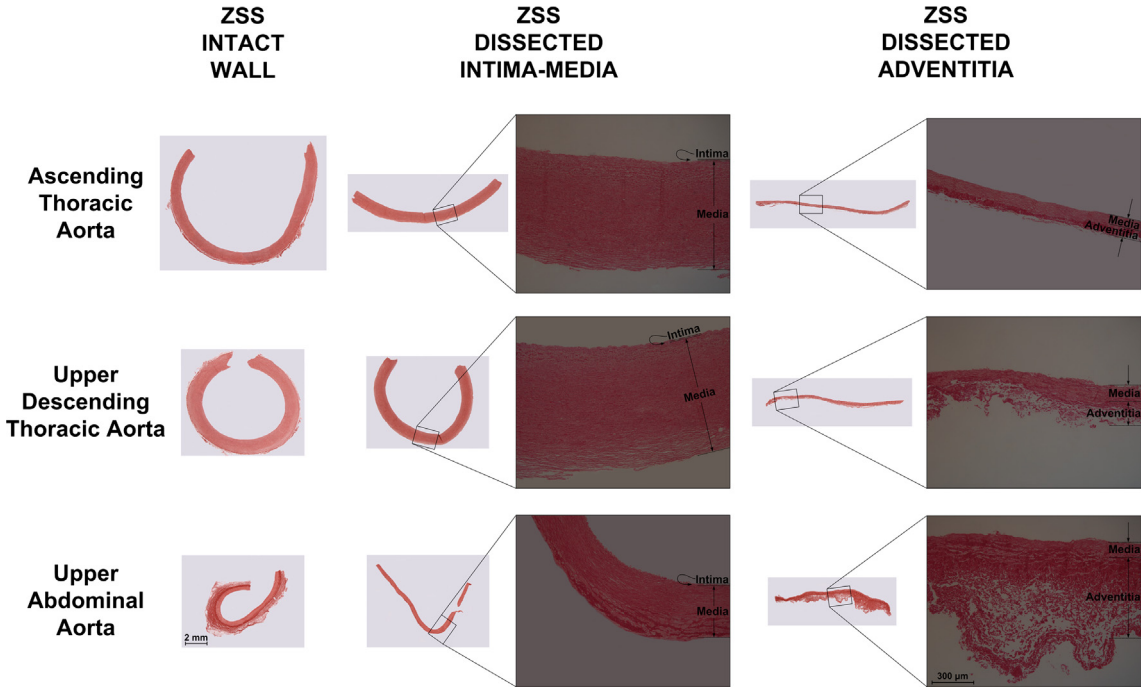

Fig. 3. Histological sections of the radially-cut (zero-stress state; ZSS) intact wall (left panel), intima-media (middle panel), and adventitia (right panel), with each row of images referring to the anatomical position indicated on the left hand side; the sections were representative but not from the same animal. Sirius red stain, staining collagen red is shown in 5-μm-thick sections. Higher magnifications (obtained with a light microscope) of the rectangular regions are shown in the insets, positioned to the right of the low magnifications (obtained with a stereomicroscope); the 2-mm scale bar applies to all the low magnifications and the 300-μm scale bar to all the higher magnifications. The images confirm that the dissection plane was always in the outermost media, with only few medial lamellar units attached to the adventitia. The smooth morphology of the dissected surfaces suggested minor traumatization of the outermost elastic lamellae. (For interpretation of the references to color in this figure legend, the reader is referred to the web version of this article.)

wall were directly based on measurements, whereas the interface between the two layers in the intact wall was estimated via an interpolation method.

3.3. Regional variations in aortic wall and layer thicknesses

Typically, the minimum and mean thickness of the intact wall at the no-load as well as at the zero-stress state decreased little along the ascending aorta and aortic arch, but reached a maximum in the upper descending thoracic aorta. It subsequently decreased rapidly along the descending thoracic aorta and remained invariant along the abdominal aorta (Fig. 5). On the other hand, the maximum thickness of the intact wall at both states showed a minor increase along the ascending aorta and a gradual decrease as the distance from the aortic origin increased. The same pattern was displayed by the corresponding thickness values of the intima-media but, contrasting the intima-media and the intact wall, the thickness of the adventitia (all three measured values) exhibited a minor change with distance from the heart. Again note that the significance of the multiple pair-wise comparisons is presented in Fig. 5. Mostly non-significant were the differences in all three thickness values between the no-load and zero-stress states, as regards the non-separated wall and its two layers. However, intimal-medial thickness was significantly greater compared with adventitial thickness in all except the abdominal positions, when examining the no-load or zero-stress state values.

3.4. Aortic wall/layer opening angles and bending-related residual stretches: regional variations

A maximum opening angle of the intact wall and intima-media was found in the ascending aorta, a minimum was found in the lower descending thoracic aorta, and then the opening angle progressively increased in more distal positions of the abdominal aorta (Fig. 6A). By contrast, the opening angle of the adventitia was invariant throughout the aorta, approaching 180 deg. In all anatomical positions, the opening angle of the adventitia was significantly greater than that of the intact wall and intima-media, with minor differences among the latter.

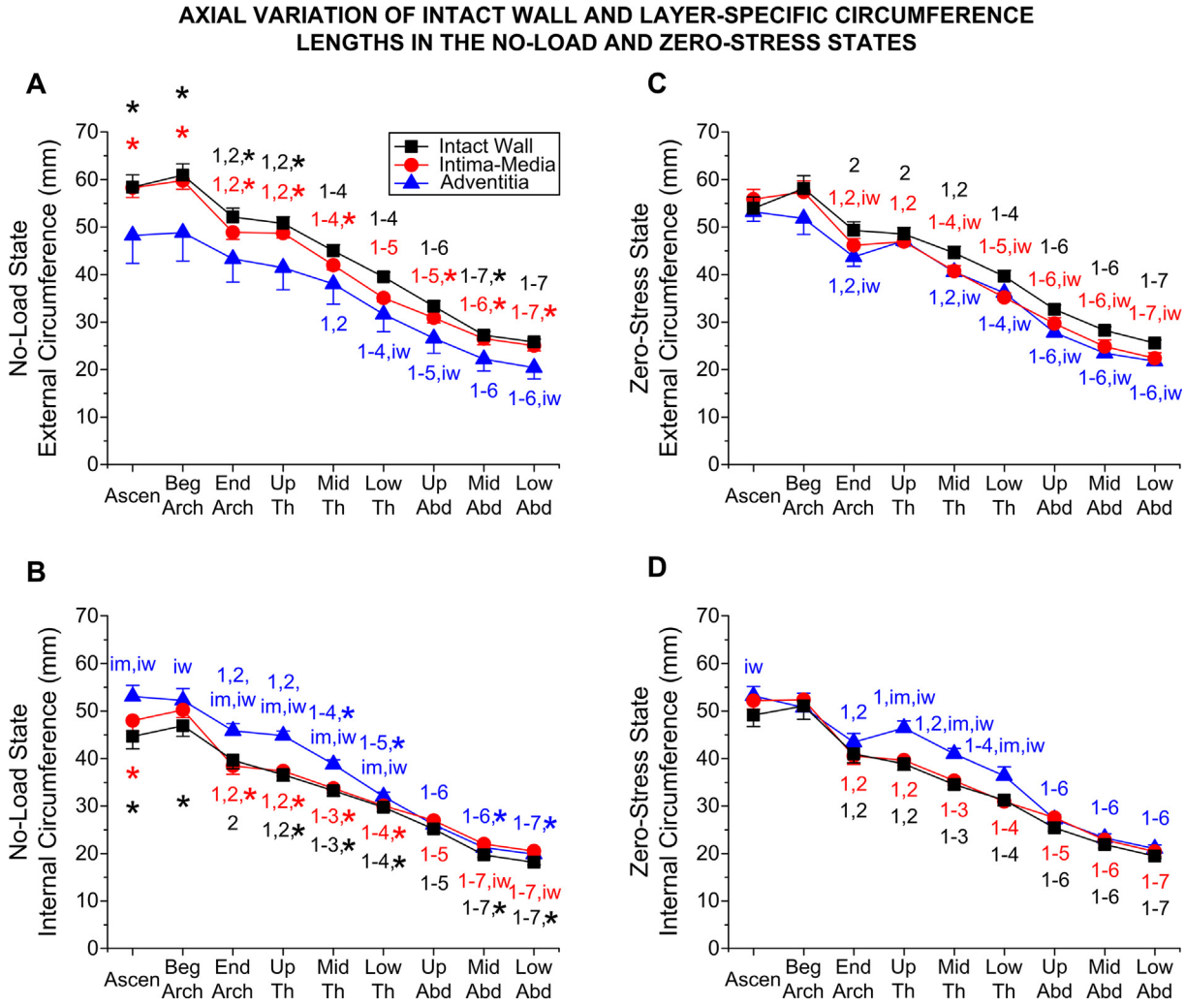

Fig. 4. (Upper) External and (lower row) internal circumference of the intact wall, intima-media, and adventitia at the no-load (A and B) and zero-stress states (C and D), shown as a function of anatomical position. These are defined as Ascen: ascending thoracic aorta; (Beg, End) Arch: beginning and end of the aortic arch; (Up, Mid, Low) Th: upper, middle, and lower descending thoracic aorta; (Up, Mid, Low) Abd: upper, middle, and lower abdominal aorta. Average values are shown and the error bars denote one standard error. Numbers 1–7 denote statistically significant differences with respect to Ascen, Beg Arch, End Arch, Up Th, Mid Th, Low Th, and Up Abd for the intact wall (black color), intima-media (red color), and adventitia (blue color), determined with one-way ANOVA for repeated measures and the Tukey post hoc test. Letters 'im' and 'iw' denote significant differences with respect to the intima-media and the intact wall in a given anatomical position, again determined with one-way ANOVA for repeated measures and the Tukey test. Symbol * denotes significant differences between the no-load and zero-stress states in a given position, determined with the paired *t*-test. (For interpretation of the references to color in this figure legend, the reader is referred to the web version of this article.)

The residual stretches released by radially cutting the rings for the intact wall and the two layers were basically tensile externally, i.e., $\left\{\lambda_{0i}^{biw}, \lambda_{0e}^{bim}, \lambda_{0i}^{ba}\right\} > 1$ and compressive internally, i.e., $\left\{\lambda_{0i}^{biw}, \lambda_{0e}^{bim}, \lambda_{0i}^{ba}\right\} < 1$ (Fig. 6(B and C)). With regard to the effect of axial position, the adventitia varied little, but, in contrast, the external residual stretch λ_{0e}^{bim} of intimal-medial rings was minimal near the diaphragm, increasing in rings taken from more distal positions and reaching a peak in the lower abdominal aorta. The smallest internal residual stretch value λ_{0i}^{bim} of intimal-medial rings occurred in the aortic root and increased as the distance from the heart increased, excluding the descending thoracic aorta, attaining

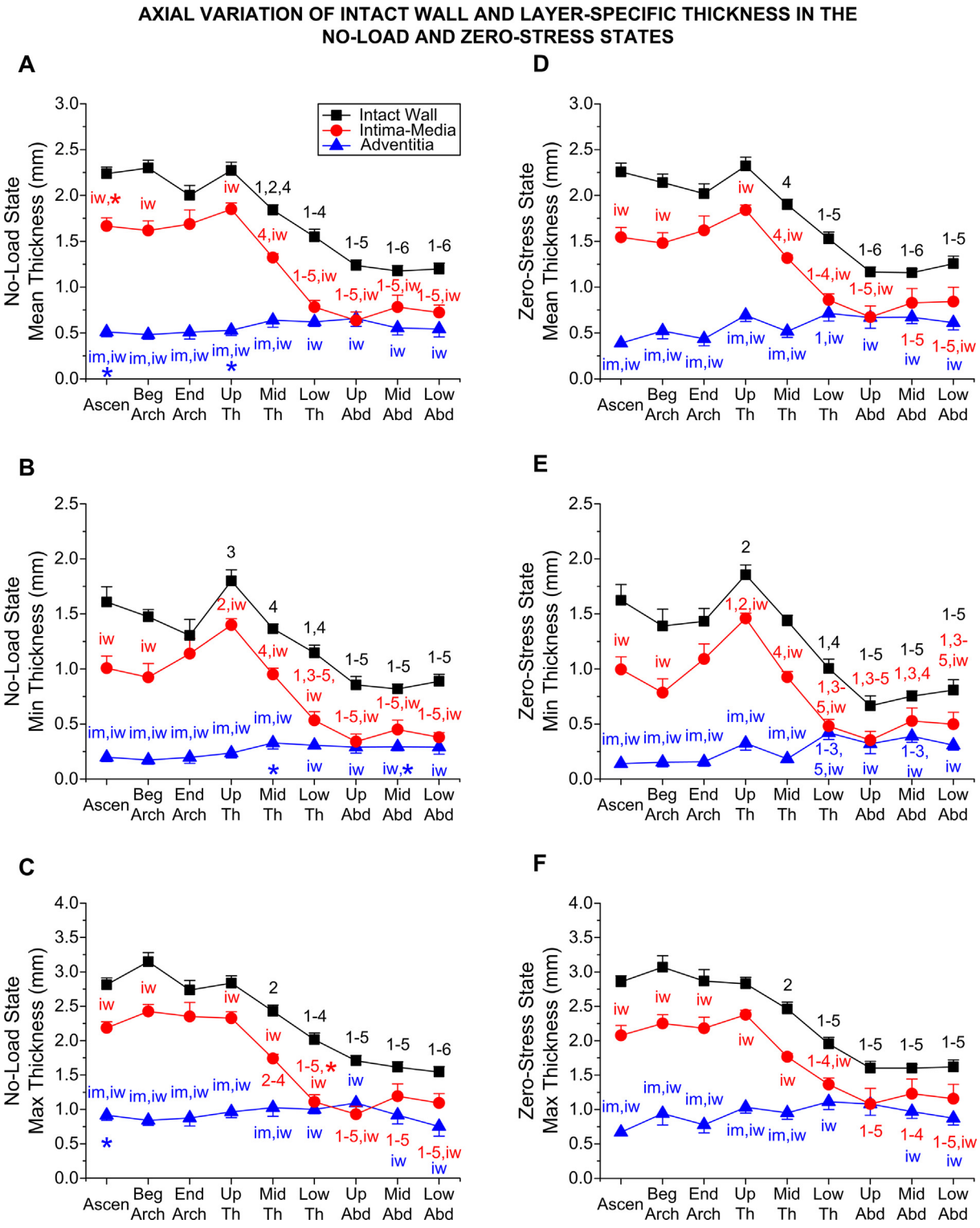

Fig. 5. Mean (upper), minimum (min; middle), and maximum (max; lower row) thickness of the intact wall, intima-media, and adventitia at the no-load (A-C) and zero-stress states (D-F), shown as a function of anatomical position. Statistical comparisons among anatomical positions and layers/intact wall, and those between the no-load and zero-stress states are summarized using numbers 1–7, letters 'im' and 'iw', and symbol * defined in Fig. 4 (error bar =±1 standard error).

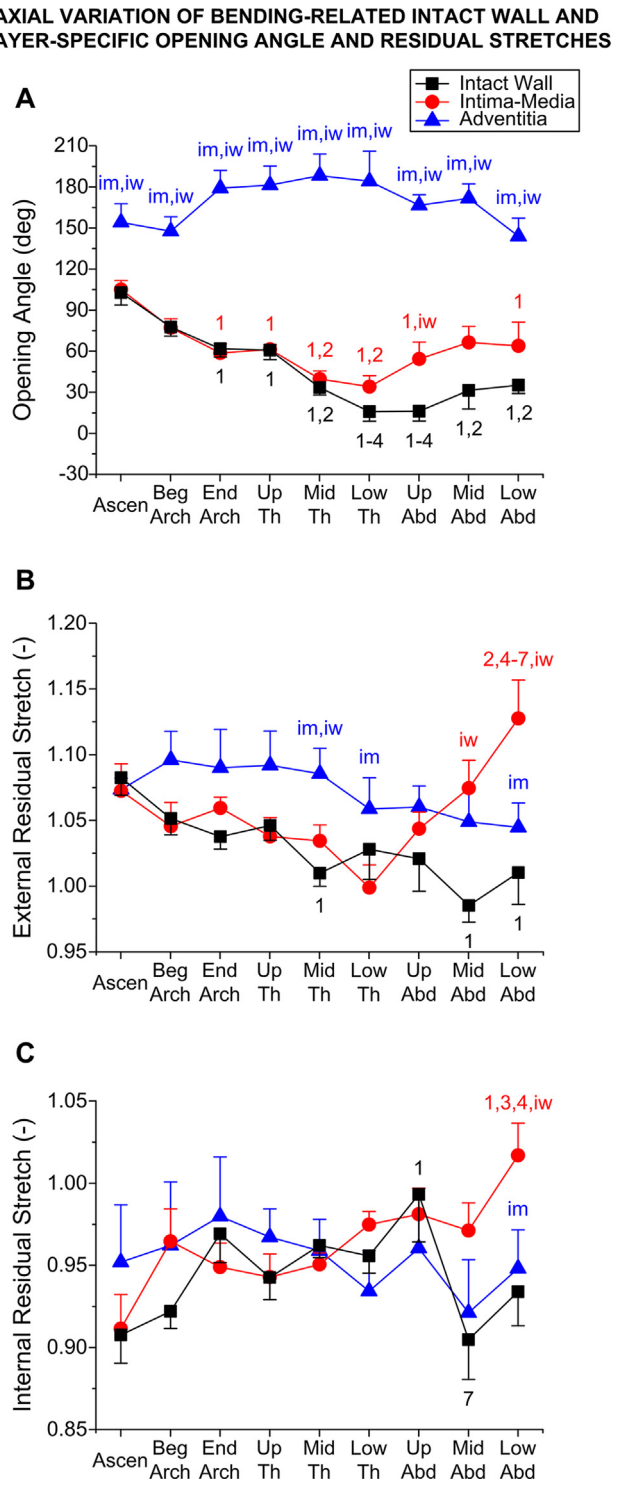

Fig. 6. (A) Opening angle of the intact wall, intimal-medial, and adventitial rings, and their corresponding (B) external and (C) internal residual stretches, shown as a function of anatomical position. Statistical comparisons among anatomical positions and layers/intact wall are summarized using numbers 1–7, and letters 'im' and 'iw' defined in Fig. 4 (error bar = ±1 standard error).

a maximum in the lower abdominal aorta. In general, the external residual stretch $\lambda_{\theta e}^{biw}$ of non-separated rings decreased along the aorta, whereas a maximum internal residual stretch $\lambda_{\theta i}^{biw}$ was observed in the upper abdominal aorta, decreasing to similar extents towards the heart and iliac artery bifurcation. Residual stretch values of intimal-medial rings were larger than those of non-separated rings, i.e., $\lambda_{\theta e}^{bim} > \lambda_{\theta e}^{biw}$ and $\lambda_{\theta i}^{bim} > \lambda_{\theta i}^{biw}$, just in the abdominal positions. The external residual stretch of adventitial were greater than those of intimal-medial rings, i.e., $\lambda_{\theta e}^{ba} > \lambda_{\theta e}^{bim}$, in the descending thoracic aorta, with the opposite trend in the lower abdominal aorta. Negligible were the internal residual stretch differences among the intact wall and its layers.

3.5. Dissection-related layer-specific residual stretches: regional variations

Tensile were both the external and internal residual stretches released in the adventitia after dissection at the no-load state, i.e., $\{\lambda_{\theta e}^{ca},\ \lambda_{\theta i}^{ca}\} > 1$ (Fig. 7(A and C)). A significant variation was found along the aorta, with the highest values in the beginning of the aortic arch, decreasing in the ascending and descending aorta, and progressively increasing towards the iliac artery bifurcation. There were non-significant differences between the external $\lambda_{\theta e}^{ca}$ and internal residual stretches $\lambda_{\theta i}^{ca}$ in any position. The residual stretches of the intima-media were generally compressive, i.e., $\left\{\lambda_{\theta e}^{cim}, \lambda_{\theta i}^{cim}\right\} < 1$, and again the external $\lambda_{\theta e}^{cim}$ and internal $\lambda_{\theta i}^{cim}$ values did not vary in any position, being maximal in the aortic arch and significantly decreasing peripherally to a minimum in the lower abdominal aorta.

Analogous results were obtained upon separating the layers from the radially-cut aortic wall, i.e., $\{\lambda_{\theta e}^{oa}, \lambda_{\theta i}^{oa}\} > 1, \left\{\lambda_{\theta e}^{oim}, \lambda_{\theta i}^{oim}\right\} < 1$ (Fig. 7(B and D)). The external $\lambda_{\theta e}^{oa}$ and internal residual stretches $\lambda_{\theta i}^{oa}$ released in the adventitia varied with position, being invariably tensile along the vessel albeit with minor differences among them. Non-significant were the differences between the external $\lambda_{\theta e}^{oim}$ and internal residual stretches $\lambda_{\theta i}^{oim}$ of the intima-media upon layer separation at the radially-cut state. Still, these values varied less clearly with axial position than their counterparts $\lambda_{\theta e}^{cim}$ and $\lambda_{\theta i}^{cim}$ at the no-load state.

4. Discussion

Evidence is submitted for the existence of significant compressive residual stretches in the intima-media and of tensile residual stretches in the adventitia that were released when the aortic wall was dissected into its two main layers. Essentially, different residual stretch values were calculated when dissecting closed rings of the aortic wall (no-load state) compared with radially-cut wall rings, typically considered as the zero-stress state ert one.for the intact wall (Fig. 7). Layer separation led to much greater opening angles in the adventitia compared with the intima-media (Fig. 6), highlighting the existence of (bending-related) layer-specific residual strains. It is also demonstrated that the opening angle of the intimal-medial layer varied with axial position on the aorta similarly with the opening angle of the intact wall. This follows the pattern presented by Han and Fung (1991), although our values are lower, possibly attributable to gender, species, and weight (female Landrace 65 kg vs. male farm 25–30 kg pigs) differences among the studies. Both studies examined youngling pigs, but their aortic diameters are smaller than ours (Fig. 4), reflecting that they used smaller and younger pigs. Note that Badreck-Amoudi et al. (1996) found that while the unloaded aortic diameter of rats increased steadily during development, the opening angle along the entire length of the aorta decreased with age until puberty, increasing thereafter as the animal matured, corroborating the reduced opening angle values for the non-separated aorta reported herein.

Our intact wall circumference/thickness data (Figs. 4 and 5) corroborate available reports on the porcine aortic geometry.

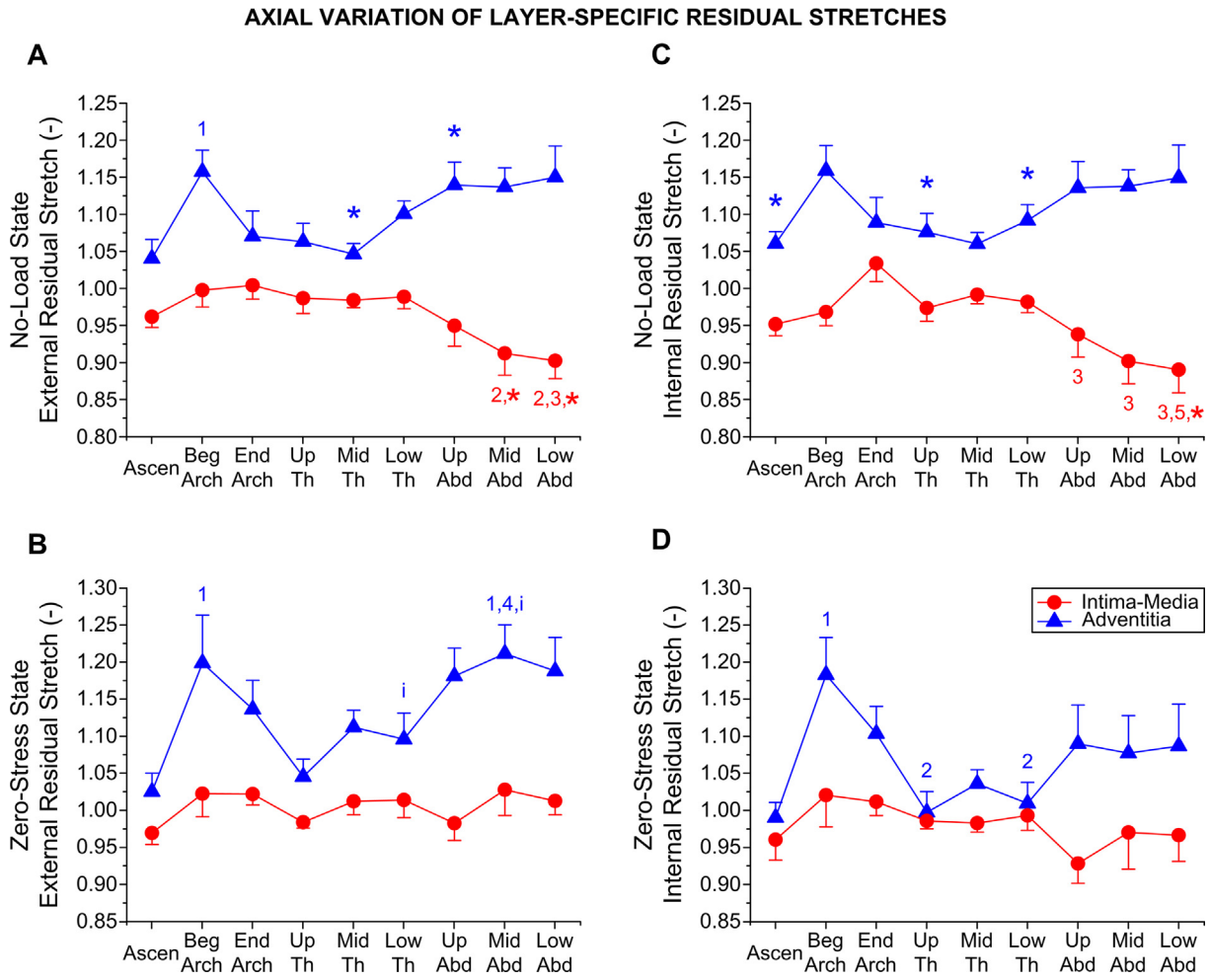

Fig. 7. Average (A and B) external and (C and D) internal residual stretches of the intima-media and adventitia relating to their dissection while at (upper panel) the no-load state and (lower panel) the zero-stress state, shown as a function of anatomical position. Letter 'i' denotes significant difference between the external and internal residual stretches in a given anatomical position, determined with the paired *t*-test. Statistical comparisons among anatomical positions and those between the no-load and zero-stress states are summarized using numbers 1–7 and symbol * defined in Fig. 4 (error bar = ±1 standard error).

Vossoughi et al. (1985) found that the mid-wall radius and average (no-load) thickness of intact aortic rings decreased linearly away from the distal end of the aortic arch. Han and Fung (1991) found that the major/minor diameters of intact rings (approximated as ellipses) decreased away from the heart, with their highest values in the arch and ascending aorta, respectively. These authors disclosed a decrease in the maximum and minimum wall thickness along the thoracic aorta and constant thickness values along the abdominal aorta, as we did, along with a maximum value yet only in minimum thickness in the upper descending thoracic aorta, consistent with our intact wall no-load data. They found that the wall was thickest on the inside of the vessel in the arch and opposite to the side where intercostal/lumbar arteries originate in the descending thoracic and abdominal aorta; unfortunately, we did not record the circumferential positions of the maximum and minimum wall/layer thicknesses.

The literature contains only few reports about aortic layer-specific opening angles and residual stretches. Holzapfel et al. (2007) documented the first ever three-dimensional residual deformations for the intact wall and the separated layers of the human abdominal aorta in the passive state. The adventitia circumferentially opened by 180 deg on average, becoming flat, whereas the intima opened slightly and the media opened similarly to the intact wall, much like our findings for the intima-media and adventitia of the entire porcine aorta. These authors reported that the media and adventitia shortened on separation by 8% and 6%, while the intima elongated by 4%. We have examined circumferential residual strains on a layer-by-layer basis; the intima was under compression, the media under tension, and the adventitia under tension in the aneurysmal abdominal aorta (Sassani et al., 2015), yet stress-free in the non-aneurysmal/aneurysmal ascending aorta (Sokolis, 2015). Peña et al. (2015), testing healthy porcine tissue, reported a smaller opening angle for the non-separated aorta and adventitia, and a greater opening angle for the intima in the proximal than the distal descending thoracic aorta. Statistical analysis of our data identified significant variations in the opening angle with anatomical position for the non-separated wall and the intima-media. Importantly, the axial distributions for the bending- and stretch-related residual deformations were significant. This is likely caused by the varying geometry (Figs. 4 and 5; Vossoughi et al., 1985; Han et al., 1991), composition (elastin content; Sokolis, 2007), and in situ axial stretch along the aorta, as has been established for the opening angle of the intact aorta in growth/remodeling models (Alford et al., 2008); see also the mathematical model by Rachev et al. (2013).

We examined the porcine aorta that resembles most the human condition and is large enough to facilitate layer separation, although several rings were discarded due to the difficulty of separating the media from the adventitia. Lu and Gregersen (2001)

and Sokolis (2010) previously obtained the zero-stress state of esophageal layers, taking advantage of the ease with which these could be separated. Remarkably like this study, the opening angle of collagen-rich mucosa-submucosa was considerably greater than that of the muscle layer; see in (Lu and Gregersen, 2001; Fig. 3) the ~180-deg opening angle of the mucosa-submucosa along rabbit esophagus and the similarly-varying opening angle of the muscle and intact wall.

Herein, the intima was not examined in isolation, because in young/healthy experimental animals it is a single endothelial cell layer resting on basal membrane that is of unimportant thickness and load-bearing capacity, while Peña et al. (2015) allowed up to six lamellar units to be attached to their intimal layers from porcine aortas. Note too that the thickness values obtained for the adventitia may be in error, due to its flimsy appearance. Higher standard errors were obtained for the layers compared with the results for the intact wall, which may be ascribed to imperfections in layer cutting or structural damage to the layers. Then again, the elastic lamellae had a physiologic appearance in our histological sections, other than few lamellae contiguous to the dissection surface (Fig. 3), so that layer separation did not appear to inflict major structural damage. Nevertheless, despite the small media portion attached to the adventitia, its contribution to the adventitial results could be significant in the proximal aorta with its rather small adventitial thickness. Furthermore, due to the limited amount of porcine tissue available for cutting axial specimens, it was not possible to examine layer-specific residual deformations in the axial direction over the whole length of the aorta. Axial residual strains have been reported for the intact porcine carotid/coronary arteries (Wang and Gleason, 2010) and human aorta (Sokolis et al., 2019). Besides, the stress-free reference configuration of layered aortic tissue was examined herein under near-passive conditions, since no chemical measures were taken to ensure that the cells were totally relaxed. Smooth muscle contraction with vasoactive substances is, however, known to affect the opening angle of the intact arterial wall (Matsumoto et al., 1996; Han et al., 2006).

Notwithstanding these limitations, the present findings indicated that the opening angle of the adventitia was near 180 deg in the different aortic positions, being systematically higher than that of the intima-media and intact wall, which were similarly distributed along the porcine aorta. Upon layer separation, compressive stretch release was evidenced in the intima-media and tensile stretch release in the adventitia that also varied with axial position. The presently-documented regional distribution of layer-specific circumferential residual strains that was hitherto unknown will help to more accurately model the aorta as a two-layer composite.

Declaration of Competing Interest

The author declares no competing interests.

Appendix A. Supplementary material

Supplementary data to this article can be found online at https://doi.org/10.1016/j.jbiomech.2019.109335.

References

Alford, P.W., Humphrey, J.D., Taber, L.A., 2008. Growth and remodeling in a thick-walled artery model: effects of spatial variations in wall constituents. Biomech. Model. Mechanobiol. 7, 245–262.

Badreck-Amoudi, A., Patel, C.K., Kane, T.P., Greenwald, S.E., 1996. The effect of age on residual strain in the rat aorta. J. Biomech. Eng. 118, 440–444.

Boudoulas, H., Wooley, C.F., 1996. Aortic function. In: Boudoulas, H., Toutouzas, P.K., Wooley, C.F. (Eds.), Functional Abnormalities of the Aorta. Futura Publishing, New York, pp. 3–36.

Chuong, C.J., Fung, Y.C., 1986. On residual stresses in arteries. J. Biomech. Eng. 108, 189–192.

Greenwald, S.E., Moore Jr., J.E., Rachev, A., Kane, T.C., Meister, J.J., 1997. Experimental investigation of the distribution of residual strains in the artery wall. J. Biomech. Eng. 119, 438–444.

Han, H.C., Fung, Y.C., 1991. Species dependence of the zero-stress state of aorta: pig versus rat. J. Biomech. Eng. 113, 446–451.

Han, H.C., Marita, S., Ku, D.N., 2006. Changes of opening angle in hypertensive and hypotensive arteries in 3-day organ culture. J. Biomech. 39, 2410–2418.

Holzapfel, G.A., Sommer, G., Auger, M., Regitnig, P., Ogden, R.W., 2007. Layer-specific 3D deformations of human aortas with non-atherosclerotic intimal thickening. Ann. Biomed. Eng. 35, 530–545.

Humphrey, J.D., 2002. Cardiovascular solid mechanics: cells, tissues, and organs. Springer-Verlag, New York.

Lu, X., Gregersen, H., 2001. Regional distribution of axial strain and circumferential residual strain in the layered rabbit esophagus. J. Biomech. 34, 225–233.

Matsumoto, T., Tsuchida, M., Sato, M., 1996. Change in intramural strain distribution in rat aorta due to smooth muscle contraction and relaxation. Am. J. Physiol. 271, H1711–H1716.

Nichols, W.W., O'Rourke, M.F., Vlachopoulos, C., 2011. McDonald's blood flow in arteries. Theoretical, experimental and clinical principles. Hodder Arnold, London.

Peña, J.A., Martínez, M.A., Peña, E., 2015. Layer-specific residual deformations and uniaxial and biaxial mechanical properties of thoracic porcine aorta. J. Mech. Behav. Biomed. Mater. 50, 55–69.

Rachev, A., Greenwald, S.E., 2003. Residual strains in conduit arteries. J. Biomech. 36, 661–670.

Rachev, A., Greenwald, S., Shazly, T., 2013. Are geometrical and structural variations along the length of the aorta governed by a principle of "optimal mechanical operation"? J. Biomech. Eng. 135, 081006-1–9.

Sassani, S.G., Kakisis, J., Tsangaris, S., Sokolis, D.P., 2015. Layer-dependent wall properties of abdominal aortic aneurysms: experimental study and material characterization. J. Mech. Behav. Biomed. Mater. 49, 141–161.

Sokolis, D.P., 2007. Passive mechanical properties and structure of the aorta: segmental analysis. Acta Physiol. 190, 277–289.

Sokolis, D.P., 2010. Strain-energy function and three-dimensional stress distribution in esophageal biomechanics. J. Biomech. 43, 2753–2764.

Sokolis, D.P., 2015. Effects of aneurysm on the directional, regional, and layer distribution of residual strains in ascending thoracic aorta. J. Mech. Behav. Biomed. Mater. 49, 141–161.

Sokolis, D.P., Savva, G.D., Papadodima, S.A., Kourkoulis, S.K., 2017. Regional distribution of circumferential residual strains in the human aorta according to age and gender. J. Mech. Behav. Biomed. Mater. 67, 87–100.

Sokolis, D.P., Bompas, A., Papadodima, S.A., Kourkoulis, S.K., 2019. Variation of axial residual strains along the course and circumference of human aorta considering age and gender. J. Biomech. Eng. 10 (1115/1), 4043877. https://doi.org/10.1115/1.4043877.

Vaishnav, R.N., Vossoughi, J., 1987. Residual stress and strain in aortic segments. J. Biomech. 20, 235–239.

Vossoughi, J., Weizsäcker, H.W., Vaishnav, R.N., 1985. Variation of aortic geometry in various animal species. Biomed. Tech. 30, 48–54.

Vossoughi, J., Hedjazi, H., Borris, F.S., 1993. Intimal residual stress and strain in large arteries. In: Langrana, N.A., Friedman, M.H., Groods, E.S. (Eds.), Proceedings of the Summer Bioengineering Conference. ASME, New York, pp. 434–437.

Wang, R., Gleason, R.L., 2010. A mechanical analysis of conduit arteries accounting for longitudinal residual strains. Ann. Biomed. Eng. 38, 1377–1387.